

# Experimental Study on Fatigue Performance of Reinforced Concrete Beams in Corrosive Environment with Cyclic Loads

Hui Wang<sup>1,2</sup>, Shiqin He<sup>1,\*</sup>, Xiaoqiang Yin<sup>3</sup> and Zeyang Cao<sup>1</sup>

<sup>1</sup>North China University of Technology, Beijing, 100144, China

<sup>2</sup>State Key Laboratory of Hydrosience and Engineering, Tsinghua University, Beijing, 100084, China

<sup>3</sup>Tianheng Group Co., Ltd., Beijing, 102442, China

\*Corresponding Author: Shiqin He. Email: heshiqin@ncut.edu.cn

Received: 12 March 2019; Accepted: 23 April 2019

**Abstract:** In marine environments, reinforced concrete bridge structures are subjected to cyclic loads and chloride ingress, which results in corrosion of the reinforcing bars, early deterioration, durability loss, and a considerable reduction in the fatigue strength. Owing to the complexity of the problem and the difficulty of testing, there are few studies on the fatigue performance of concrete structures under the combined action of corrosion environment and cyclic load. Therefore, a coupling test device for corrosion and cyclic load is designed and fatigue tests of reinforced concrete beams in air environments and chlorine salt corrosive environments are carried out. The fatigue corrosion process, damage mode, and corrosion features of the test beams as well as chloride ion content in concrete are analyzed. The relationships of deflection, crack, and number of cycles in the different environments are given. Results show that the fatigue life of the beam is greatly reduced under coupled effects of the cyclic load and corrosive environment, the failure form of the beam is corrosion fatigue damage. The deflection and crack keeps growing with the increase in loading cycles. Under the coupling of cyclic load and corrosion environment, the content of chloride ion in concrete is low and there is less variety along the direction of penetration.

**Keywords:** Reinforced concrete; cyclic load; corrosion fatigue; coupled effect; fatigue life; chloride ion content

## 1 Introduction

Despite the rapid development of new materials, reinforced concrete is still widely used in offshore engineering. In recent years, the collapses of cross-sea bridges and railways have shown that serious durability problems exist in offshore reinforced concrete structures [1,2]. During their service life, Coastal concrete structures, like roads, railways, and bridges, are subjected to dynamic loading from vehicles and the atmospheric marine environment at the same time. The failure mode is a kind of fatigue failure that is induced by the coupled action of cyclic loads and a corrosive environment [3–5]. Series of research works have been carried out to investigate the durability of concrete structures under the combination of constant loads and a corrosive environment [6–12]. However, previous studies mainly investigated the



This work is licensed under a Creative Commons Attribution 4.0 International License, which permits unrestricted use, distribution, and reproduction in any medium, provided the original work is properly cited.

effects of simultaneous load and steel corrosion on the corrosion rates and the mechanical behaviour of RC structures. Previous study show that the simultaneous corrosion and load may significantly increase deflections of RC beams. But due to the different test details, contrasting results of the coupled effects on the corrosion rate and the crack widths may got.

Studies on the interaction of cyclic load and corrosive environment have mostly focused on the fatigue properties of reinforced concrete beams with different corrosion degrees of steel bars based on a accelerated corrosion method. The steel bars were accelerated to corrode before loading [13–19]. From these studies, the main problems are: firstly, reinforcement corrosion in RC structures was accelerated by electric current, which is a different phenomenon from that of the corrosion of steel in an actual engineering corrosion environment. In general, steel corroded by electricity is evenly rusted, whereas that corroded in natural environments is pitting [20]; secondly, in practical engineering, corrosion and load were taken place in the same time. The behavior of beams that are corroded under simultaneous cyclic load and steel corrosion is expected to be different to the behavior of beams based in sequential corrosion and cyclic load application. Whereas studies coupling a corrosive environment and fatigue coupling are relatively few [21–24]. Although the coupling of corrosion and fatigue tests can be achieved by artificial simulated conditions of climate, the cost is high.

The coupling of corrosion and fatigue tests in this study were designed and achieved by spraying chloride solution and applying the cyclic load at the same time. The test of flexural reinforced concrete beams was carried out, and the deformation properties and fatigue life of the concrete beam as well as chloride ion content in concrete were studied, which provide insights for the evaluation of fatigue damage and life prediction of reinforced concrete structures in corrosive environments.

## 2 Test Program

Five prismatic reinforced concrete beams were designed and cast in this test. The reinforcement configuration is shown in Fig. 1. Longitudinal tensile steel bars were of 12-mm diameter and had yield strengths of 420 MPa and ultimate strengths of 583 MPa. Compression steel bars were of 10-mm diameter. Stirrups were steel bars of 8-mm diameter spaced at 100-mm intervals within the shear span of 700 mm. In the moment span of 500 mm, neither stirrups nor compression steel bars was used. The cover

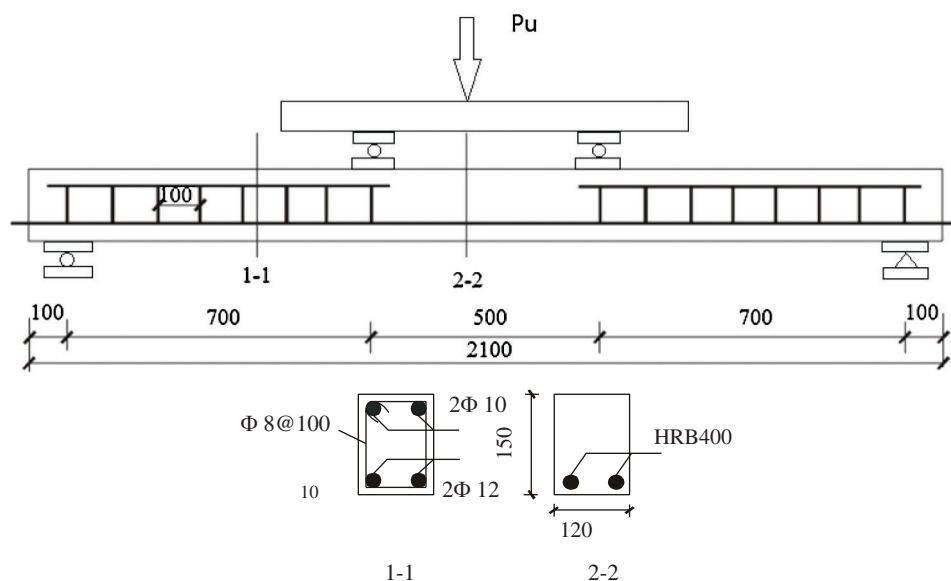


**Figure 1:** Geometry and reinforcement information of test specimens (mm)

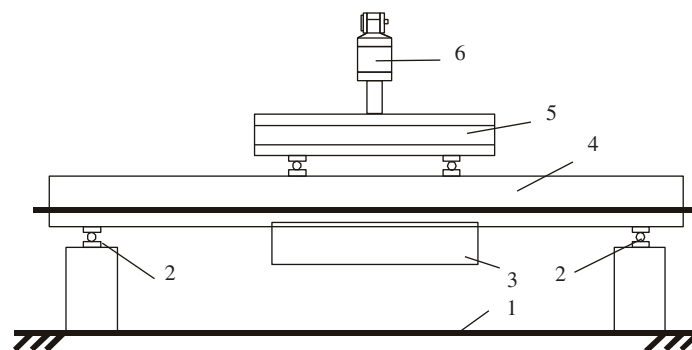
of the reinforcing steel was 23 mm in thickness. The 28-day average cubic (100 mm × 100 mm × 100 mm) compressive strength was tested to be 36.7 MPa, and increased during the curing process, reaching 50 MPa at 70 d. The strength remained constant until the specimens were loaded. All test specimens were loaded under four-point bending.

The test plan is shown in Tab. 1. Specimen C-0 is a static load damage beam to determine the ultimate bearing capacity. Specimen C-1 is a comparison beam for fatigue damage to determine the fatigue life of the beam in atmospheric environment. Specimens C-2, C-3, and C-4 are the test beams for the coupling of cyclic load and corrosive environment.

**Table 1:** Test plan

Specimen number	Test method	Loading amplitude	Loading frequency/Hz
C-0	Static load until damaged	–	–
C-1	Cyclic load + Air environment	7%–70% $P_u$	2
C-2	Cyclic load + Corrosive environment	7%–70% $P_u$	1
C-3	Cyclic load + Corrosive environment	7%–70% $P_u$	1
C-4	Cyclic load + Corrosive environment	5%–50% $P_u$	1

A schematic of the coupling of corrosion and fatigue test setup is shown in Fig. 2. The device has many advantages such as simple, easy production and high cost performance. The loads were applied by the electro-hydraulic servo loading actuator (6), which could be adjusted to meet different load requirements. A plexiglas tank (3) was positioned on the bottom of the moment span, while the PVC pipes were installed to pump the chloride solution from the tank and spray on continuously during the process of fatigue. When spraying continuously or discontinuously, the device can simulate different marine environments such as underwater zone, splash zone, fluctuating water level zone or wet-dry cycling zone. The rust of the steel bars in concrete caused in the simulated marine environment was similar to that of in a natural environment.



1- Strong floor 2- Simple-supported support 3- Plexiglas tank; 4- RC test beam 5- Load distributor 6- Loading actuators

**Figure 2:** Loading system for coupling of corrosion and fatigue tests

The corrosion and cyclic load coupling test is shown in Fig. 3. At the bottom of moment span, the PVC pipes were installed to pump the chloride solution of 3.5% from the tank and spray on continuously during the process of fatigue. The fatigue test load was equal amplitude repeated loading controlled by the electro-hydraulic servo system. The ultimate bearing capacity of the beam was  $P_u = 30$  kN, measured in the static



**Figure 3:** Corrosion fatigue coupling test method

load test. The fatigue test process began with three static loads, starting from 0 kN and loading to the upper limit. Then the cyclic load was applied and the load varied in sine. The fatigue damage was marked by the break of the longitudinal bar or the width of the crack exceeding 2 mm. The process was stopped when the cyclic load cycle reached a certain number of times, after which the data collecting of static load cycle and observation recording deflection and fracture were performed.

As shown in Fig. 4, the dial indicators were arranged in the span, the supporting position and the loading point. The strain gauges were pasted across the middle of the beam. The clip extensometers were arranged to measure the width of the crack at the loading point of the beam. The data was automatically collected by DH3820 with a frequency of 50 Hz.

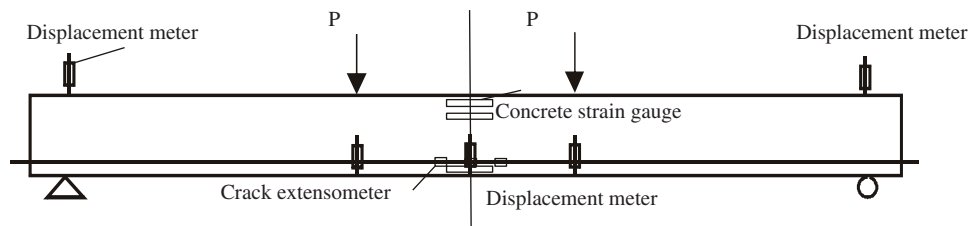


**Figure 4:** Location of measuring points

### 3 Test Results and Analysis

#### 3.1 Fatigue Life and Failure Form

Tab. 2 summarizes the fatigue test result of specimens. When the cyclic load level was  $\sigma_{\max}/\sigma_u = 0.7$ , the fatigue life of specimen C-1 in air environment was 418,012 times, while the fatigue lives of specimens C-2 and C-3 under corrosion and fatigue coupling were 198,023 times and 166,054 times, respectively. Thus, the fatigue lives of specimens C-2 and C-3 were reduced by 53% and 60%, respectively, compared to the fatigue life of specimen C-1. The result shows that chlorine corrosion and cyclic load coupling had a great influence on the fatigue life of beam. When the cyclic load level was  $\sigma_{\max}/\sigma_u = 0.5$ , the fatigue life of specimen C-4 under the corrosion and fatigue coupling was 1,268,145 times.

Fig. 5 presents the failure form of each specimen. The failure form of static load specimen C-0 was a typical damage of reinforced beam, and other fatigue test specimens were damaged with bars broken. When the cyclic load reached 418,012 times, a tensile steel bar of specimen C-1 broke at one of the loading points, and the concrete was completely crushed and dislocated, indicating the test beam was

**Table 2:** Results of corrosion fatigue test

Specimen number	Test environment	Load amplitude (kN)	Frequency (Hz)	Fatigue life (times)	Corrosion fatigue time (h)	Failure form
C-1	Air environment	7%–70%Pu	2	418012	116	1 bar broken
C-2	Corrosion environment	7%–70%Pu	1	198023	55	2 bars broken
C-3	Corrosion environment	7%–70%Pu	1	166054	46	1 bar broken
C-4	Corrosion environment	5%–50%Pu	1	1268145	352	1 bar broken

damaged. When the cyclic load reached 198,023 times, the specimen C-2 was suddenly broken into two parts from one of the loading points, with both of two tensile steel bars broken. When the cyclic load of specimen C-3 reached 166,054 times, a large fracture occurred at the bottom of a loading point, with the deflection increasing greatly, indicating the fracture of a steel bar. After the beam was removed, the crack smashed and the tensile reinforcement was exposed broken. When the cyclic load reached 1,268,145 times, the concrete in the bottom of the beam was cracked, indicating the fracture of a steel bar. After the beam was removed, the crack was smashed, and the tensile reinforcement was observed to be broken.

### 3.2 Deflection-Load Curves and Deflection-Load Cycle Times Curves

Fig. 6 shows the deflection-load curves and midspan deflection-load cycle times curves of specimens. During the fatigue process, the deflection of the beam increased along with the loading and unloading, indicating that the fatigue damage was a cumulative process. The residual deformation mainly occurred in the previous load cycle, but the residual deformation of the same load cycle decreased gradually as the number of load cycles increased. After the initial static load of three times, the maximum deflection of specimen C-1 was 9.77 mm. With the increase of the load cycles, the maximum deflection was also increasing. The maximum deflection increased by 1.81 mm after the cycle of 360,000. Before the specimen was damaged, the maximum deflection was 11.60 mm. The maximum deflection of specimen C-3 was 8.34 mm after the initial static load of three times, and the maximum deflection increased by 1.55 mm after the cycle of 130,000. Before the fracture, the crack width and the deflection increased a lot. The maximum deflection of specimen C-4 was 6.08 mm after the initial static load of three times, and the maximum deflection increased by 0.75 mm after the cycle of 1,300,000. Before the specimen was broken, the maximum deflection was 6.83 mm.

The midspan deflection-load cycle times (lgN) curves show that, the front and back sections of slow-deflection-growth are short, while the middle section of rapid-deflection-growth is relatively long. Although the fatigue life of each specimen is different, the deflection development laws corresponding to different load levels are basically the same. Under the cyclic load, the midspan deflection increased with the increase of the number of load cycles, and the growth rate under different load levels and environment varied.

Compared with the maximum midspan-deflection of the specimen after 1,000 times load cycles, the relationship between the growth rate of deflection and the number of load cycle times was obtained, as shown in Fig. 7. Due to the large dispersion of the fatigue test, the deflection growth rate of specimens was different. Fig. 7a shows that the deflection growth curve of specimens in corrosive environment was steeper than the specimens in air environment, indicating that the corrosive environment accelerated the

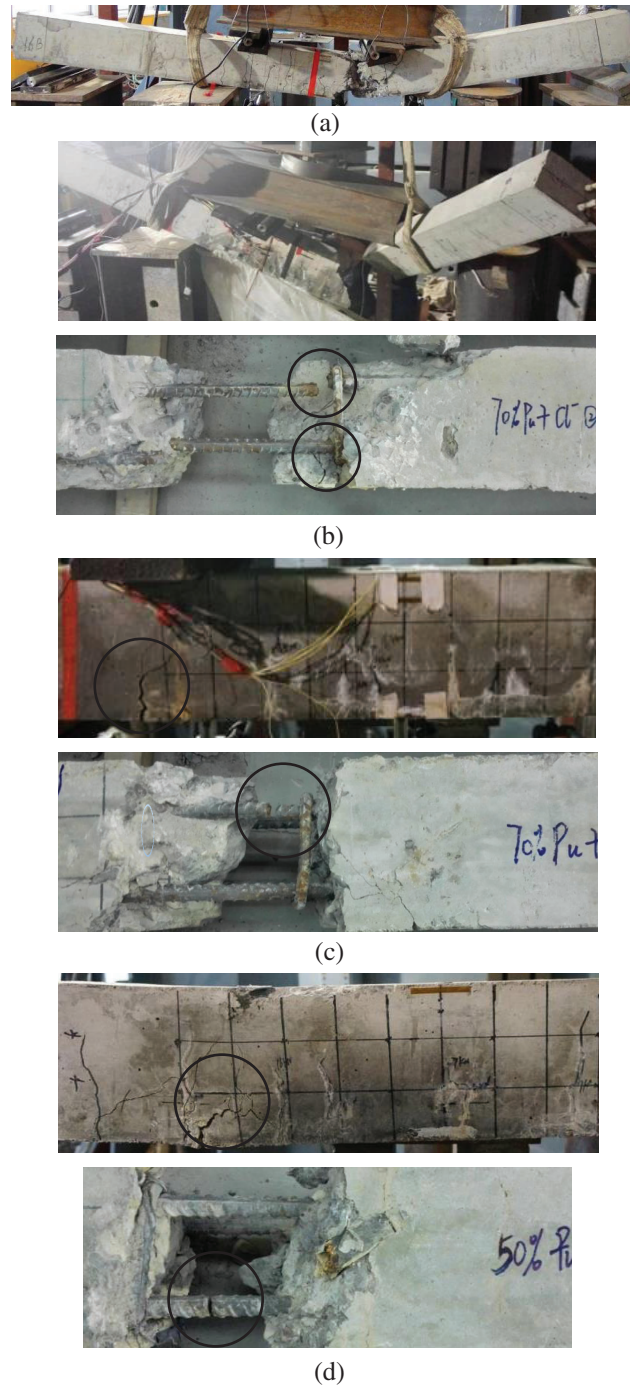


**Figure 5:** Failure form of each tested beam (a) Failure form of C-1 (b) Failure form of C-2 (c) Failure form of C-3 (d) Failure form of C-4

accumulation and development of corrosion fatigue damage. Fig. 7b presents the deflection-load cycle times curves of specimens in corrosive environment. The deflection growth rate of specimens with high stress level ( $\sigma_{\max}/\sigma_u = 0.7$ ) was higher, whereas the fatigue life was longer for the specimens with lower stress level

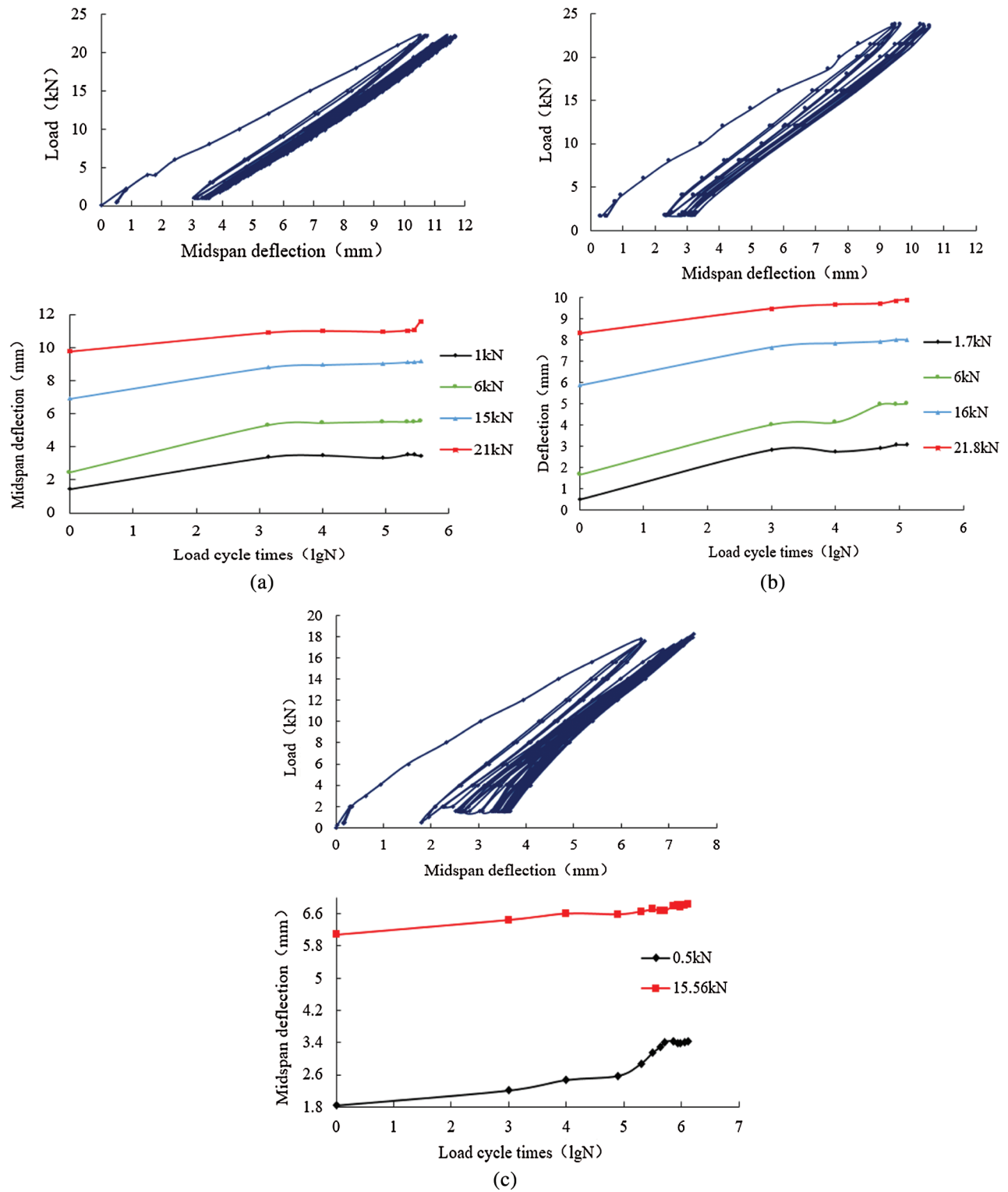


**Figure 6:** Deflection-load curves and midspan deflection-load cycle times curves (a) Specimen C-1 (b) Specimen C-3 (c) Specimen C-4

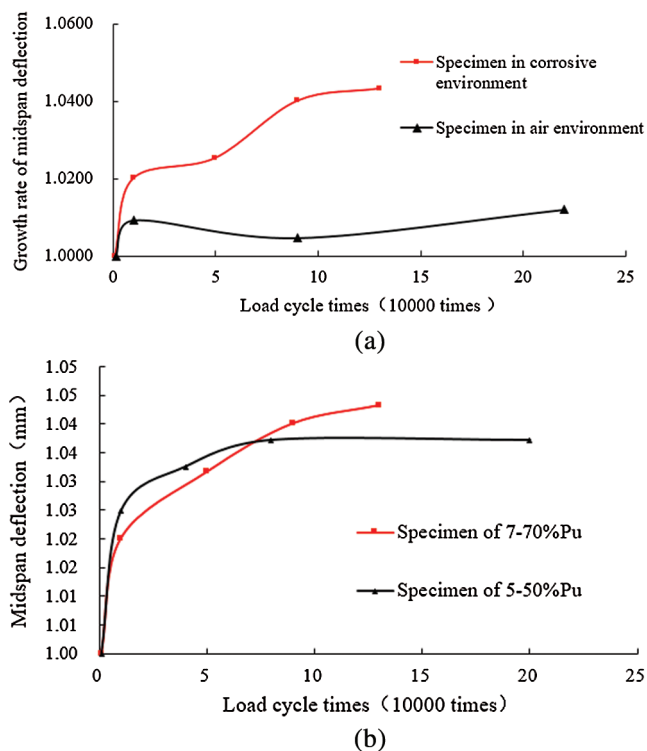


**Figure 7:** Deflection growth rate-load cycle times curves (a) Specimens of  $\sigma_{\max}/\sigma_u = 0.7$  (b) Specimens in corrosive environment

( $\sigma_{\max}/\sigma_u = 0.5$ ) and the growth rate of the deflection was relatively gentle, which shows that the fatigue stress level has a great influence on fatigue life and fatigue performance in corrosive environment.

### 3.3 Relationship between Fracture Development and Load Cycle Times

The first crack of each specimen appeared when the load reached about 3–4 kN. There were about 7 cracks in the moment span of each specimen, and the spacing of each crack was 60–100 mm. The crack width increased gradually during the fatigue process, but the increase was small before the beam was broken thoroughly, with no new crack appearing. Before specimen C-3 was broken, longitudinal cracks began to appear at the end of transverse cracks, indicating that the bond between the reinforced concrete and the concrete was damaged due to the coupling effect of corrosion fatigue. Fig. 8 shows the relationship between the width of a crack near the loading point and the load cycles. With the increase of the number of load cycles, the crack width in upper and lower limits of load increased slowly, and the width of overall increase was small, with an average increase about 0.04 mm. The crack had a residual width after the fatigue test.

### 3.4 Relationship between Concrete Strain and Load Cycle Times

Fig. 9 presents the relationship of the concrete maximum compressive strain in the compression zone and load cycle. Before specimen C-1 was damaged, the maximum strain was  $-763 \mu\epsilon$  and the maximum residual strain was  $-190 \mu\epsilon$ . Before specimen C-3 was damaged, the maximum strain was  $-885 \mu\epsilon$  and the maximum residual strain was  $-185 \mu\epsilon$ . Before the failure, the initial strain was increased. Compared with the concrete strain of specimens C-1 and C-3, the specimen in chlorine environment had the maximum strain. The curve of concrete strain-load cycle times was steady, indicating that the

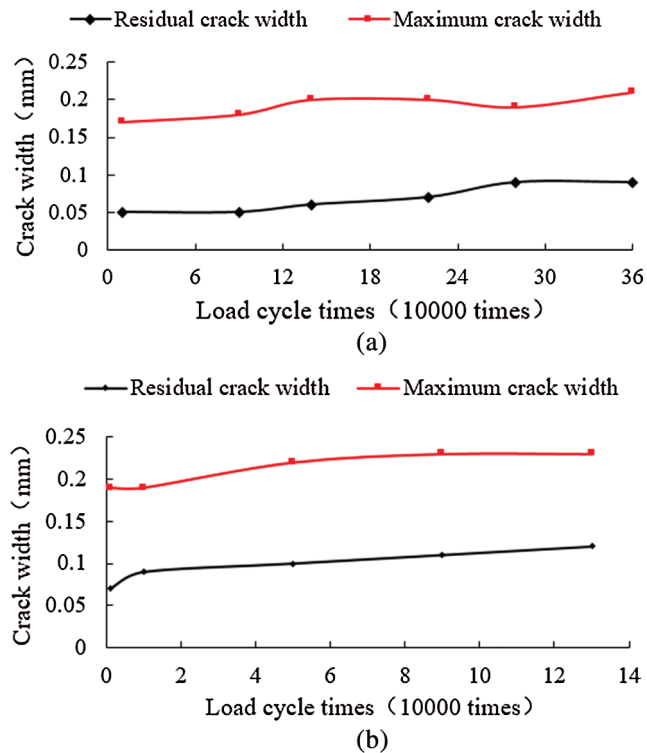


**Figure 8:** Crack development-load cycle times curves (a) Specimen C-1 (b) Specimen C-3

accumulation of concrete damage in the process of cyclic load was slow. Damage of a specimen was mainly caused by the fatigue fracture of steel bars.

### 3.5 Analysis and Comparison of Chloride Content in Concrete

After the fatigue testing, the free chloride ion content at crack sections and sections between cracks were tested. The results are shown in Figs. 10 and 11. The chloride ion content in the figure is the percentage of free chloride ion in concrete mass. Meanwhile, a batch of reinforced concrete beams were cast to carry out the experiment under a sustained load in a chloride salt corrosive environment. The sustained loads were 52% and 67% of  $P_u$ , respectively, and the loading time was 240 d and 360 d. The tested beams were unloaded and removed after reaching the designed loading time. Then, the free chloride ion content of the concrete at crack section and at sections between cracks was tested with the same method [25]. The test results were also shown in Figs. 10 and 11.

Fig. 10 shows the results of beams under 50%  $P_u$  loading. It can be seen that for the beams under sustained load, 50%  $P_u$ -360 d and 50%  $P_u$ -240 d, the free chloride content was the largest on the concrete surface. As the distance from the surface increases, the content decreases gradually. The free chloride content of the beam of loading time 360 d was greater than that of 240 d at the same depth, which indicated that the chloride content increased with the test time. However, due to the short test time for the beam in a corrosion environment with cyclic load (352 h), the free chloride content is relatively low at all depths and is almost unchanged in the depth direction. Comparing Figs. 10a, 10b, the free chloride ion content in each layer of concrete at crack section is larger than that at sections between cracks for the beam under sustained load and corrosion environment, which indicated that the cracking can accelerate the penetration of chloride ions. Whereas, the free chloride ion content at crack section and at sections between cracks is not much different for beam C4 under cyclic load and corrosion environment. Fig. 11

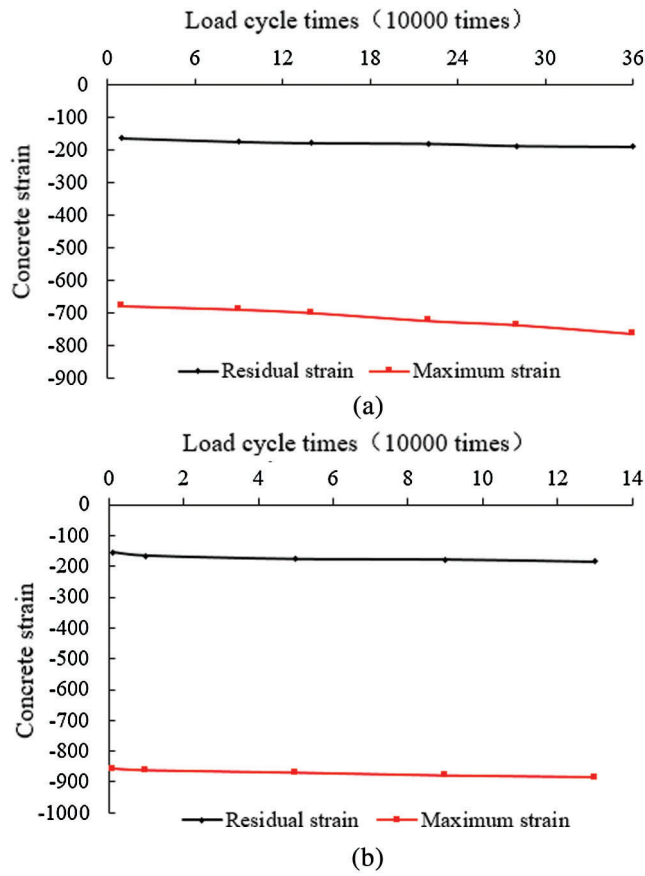


Figure 9: Concrete strain-load cycle times curves (a) Beam C-1 (b) Beam C-3

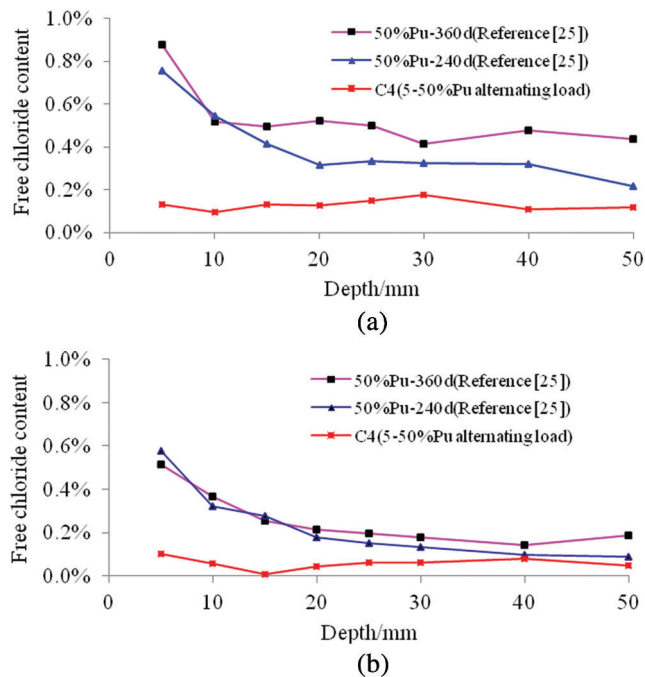
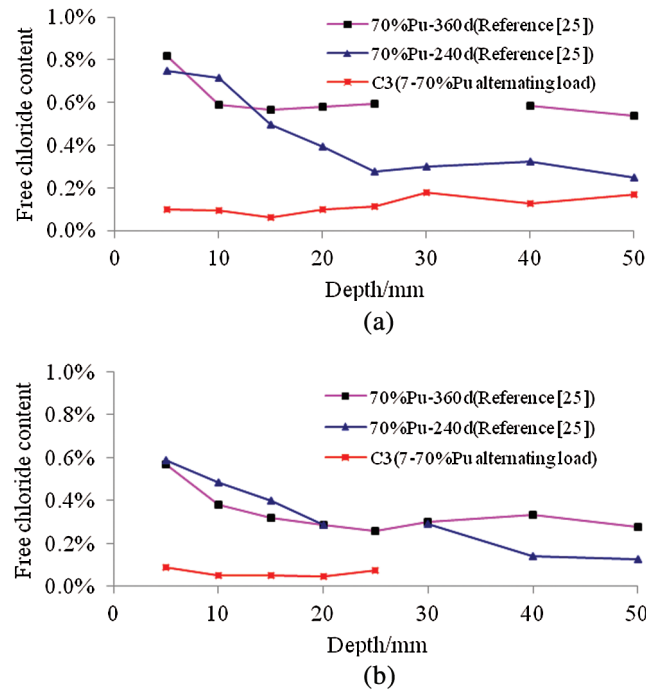


Figure 10: Free chloride content profiles with depth under 50%  $P_u$  loading (a) crack section (b) Section between cracks



**Figure 11:** Free chloride content profiles with depth under 70%  $P_u$  loading (a) crack section (b) Section between cracks

shows the results of beams under 70%  $P_u$  loading. The chloride ion permeation law was the same as the beam under 50%  $P_u$  as shown in Fig. 10.

### 3.6 Analysis of Corrosion Fatigue Characteristics of Reinforced Concrete Beams

Compared with the specimen C-1 in air environment, the fatigue life of specimens C-2 and C-3 were greatly reduced, which indicated that the corrosion medium had a great influence on the fatigue performance of components. The fatigue failure characteristics of the reinforced concrete components under the coupling of corrosion and cyclic load were different from the fatigue characteristics in the air. In the fatigue test, the crack opened and closed with the cyclic load cycle. For specimens in corrosive environment, as shown in Fig. 12, since the NaCl solution was continuously flowing into the beam through the crack, the crack was formed into a negative pressure vacuum during the opening and closing, so that the NaCl solution was drawn and extruded from the crack, and the extruded NaCl solution was mixed with bubbles. After a certain number of cycles, there were white substances around the cracks. After a period of fatigue, the surface of the white substances appeared with rust, indicating that the rebar was corroded and the rust was precipitated out from the crack with the chloride solution.

As the concrete in the tension region was cracked, the crack width was large at the loading point especially, where the stress concentration was more likely to appear, leading to the fatigue crack of the steel. The rebar and chlorine salt solution were in direct contact during the fatigue process, which is more likely to create pits and increase the defects of steel, contributing to the formation of fatigue cracks. The ultimate fatigue fracture of specimen appeared at the position of cracks near the loading point, and the fatigue life was greatly reduced.

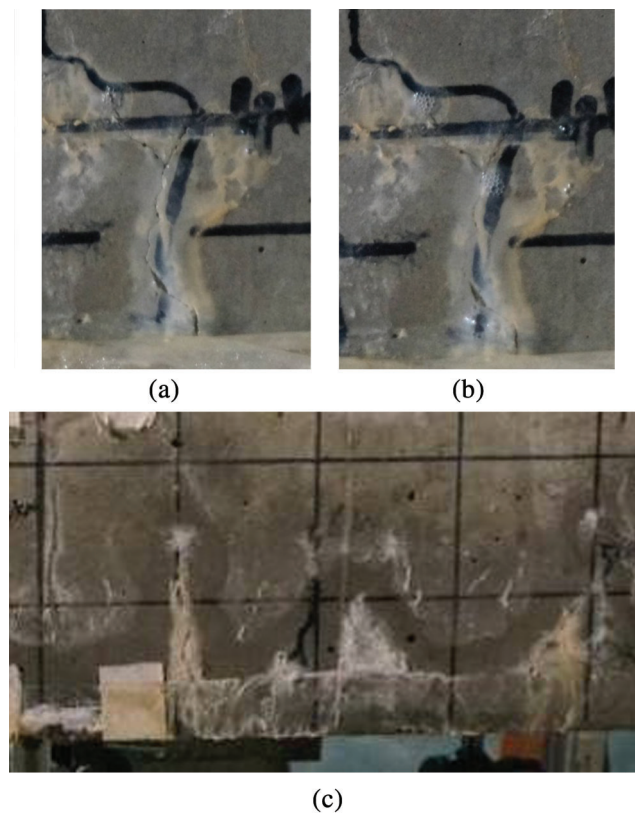


**Figure 12:** Phenomenon of cracks in corrosion fatigue specimen (a) Crack opening (b) Crack closing (c) The formation of white rust material

#### 4 Conclusions

(1) The fatigue damage process of all specimens was basically consistent, and the modes of fatigue failure were the same, but the rates of damage development varied. The fatigue damage occurred at the crack position of the loading point, indicating that the fracture under the cyclic load was related to stress concentration and the degree of corrosion of the rebar. The life of the two fatigue specimens in the corrosive environment decreased by 60% and 57.3% compared with the specimen in the air environment. Load level, a corrosive environment and the coupling between them are the main factors affecting fatigue life.

(2) When the cyclic load level was 7%–70% $P_u$ , the deflection growth rate of the specimen in the corrosive environment was higher than that of the specimen in the air environment, indicating that the damage accumulation and development of the specimen were accelerated by chlorine corrosion. When the corrosive environment was the same, the deflection growth rate of the specimen under 7%–70% $P_u$  was higher than that of the specimen under 5%–50% $P_u$ , indicating that the stress level increase can also accelerate the damage accumulation and development of the specimen. The width of the cracks widened as the load cycle number increased.

(3) A negative pressure vacuum area existed in the beam under the coupled effect of cyclic loading and corrosion environment. The vacuum area were caused by the extrusion of a mixture of gas and water on the crack surface and will lead to the corrosion of the salt and steel. The results show that the spraying equipment used in this research is feasible to simulate the ocean environment The fatigue fracture of the specimen was caused by the coupling of the cyclic load and a corrosive environment, and the coupling mechanism needs to be further studied.

(4) Under the coupling of cyclic load and corrosion environment, the content of chloride ion in concrete is low, and there was less variety along the direction of penetration. While under the coupling of sustained load and corrosive environment, the chloride ion content in concrete was relatively high and gradually decreased along the direction of penetration. The chloride ion in the concrete at crack section was higher than that at section between cracks, indicating that the crack accelerated the diffusion rate of chloride ion in the concrete.

**Acknowledgement:** The authors are grateful for the financial support provided by Open Research Fund Program of State key Laboratory of Hydrosience and Engineering. Also we would like to thank LetPub (www.letpub.com) for providing linguistic assistance during the preparation of this manuscript.

**Funding Statement:** The author(s) received funding for this study from Open Research Fund Program of State key Laboratory of Hydrosience and Engineering (No. sklhse-2018-C-05).

**Conflicts of Interest:** The authors declare that they have no conflicts of interest to report regarding the present study.

## References

1. Maaddawy, E. T., Soudki, K., Topper, T. (2005). Long-term performance of corrosion-damaged reinforced concrete beams. *ACI Structural Journal*, 102(5), 649–656.
2. Goitseone, M., Alexander, M., Moyo, P. (2009). Steel corrosion on RC structures under sustained loads—a critical review. *Engineering Structures*, 31(11), 2518–2525. DOI 10.1016/j.engstruct.2009.07.016.
3. Ahn, W., Reddy, D. V. (2001). Galvanostatic testing for the durability of marine concrete under fatigue loading. *Cement and Concrete Research*, 31(3), 343–349. DOI 10.1016/S0008-8846(00)00506-8.
4. Emilio, B. (2018). Reliability of reinforced concrete structures subjected to corrosion-fatigue and climate change. *International Journal of Concrete Structures and Materials*, 12(1), 1–13. DOI 10.1186/s40069-018-0237-8.
5. Yang, H., He, H. X., Yan, W. M. (2019). Time-varying bearing capacity evaluation of bridge under coupling action of corrosion and fatigue. *Engineering Mechanics*, 36(02), 165–176. DOI 10.6052/j.issn.1000-4750.2017.12.0940.
6. Goitseone, M., Mark, A. (2010). Lateral deformation of RC beams under simultaneous load and steel corrosion. *Construction and Building Materials*, 24(1), 17–24. DOI 10.1016/j.conbuildmat.2009.08.005.
7. Hariche, L., Ballim, Y., Bouhicha, M., Kenai, S. (2012). Effects of reinforcement configuration and sustained load on the behavior of reinforced concrete beams affected by reinforcing steel corrosion. *Cement and Concrete Composites*, 34(10), 1202–1209. DOI 10.1016/j.cemconcomp.2012.07.010.
8. He, S. Q., Gong, J. X., Zhao, G. F. (2005). Experimental investigation on durability of reinforced concrete beam in a simulated marine environment. *China Ocean Engineering*, 19(1), 11–20.
9. Li, Y., Yang, D. W., Zhang, J. K. (2018). Durability of reinforced concrete structures under coupling action of load and chlorine erosion. *Structural Durability & Health Monitoring*, 12(1), 51–63.
10. Li, P. F., He, S. Q. (2018). Effects of variable humidity on the creep behavior of concrete and the long-term deflection of RC beams. *Advances in Civil Engineering*, 10, 1–12.
11. Vidal, T., Castel, A., Francois, R. (2007). Corrosion process and structural performance of a 17 years old reinforced concrete beam stored in Chloride environment. *Cement and Concrete Research*, 37(11), 1551–1561. DOI 10.1016/j.cemconres.2007.08.004.
12. Yoon, S., Wang, K., Weiss, J., Shah, S. (2009). Interaction between loading, corrosion, and serviceability of reinforced concrete. *ACI Materials Journal*, 97(6), 737–644.
13. Ma, Y. F., Su, X. C., Guo, Z. Z., Wang, L., Zhang, J. R. (2017). Experimental study on fatigue behavior of reinforced concrete beams with corrosion induced cracking. *Journal of Natural Disasters*, 26(06), 61–68.
14. Niu, D. T., Miao, Y. Y. (2018). Experimental study on fatigue performance of corroded highway bridges based on vehicle loading. *China Civil Engineering Journal*, 51(03), 1–10.

15. Sun, J. Z., Huang, Q., Ren, Y. (2015). Performance deterioration of corroded RC beams and reinforcing bars under repeated loading. *Construction and Building Materials*, 96, 404–415. DOI 10.1016/j.conbuildmat.2015.08.066.
16. Wu, J., Wang, C. X., Xu, J. (2012). Study on flexural behavior of corroded reinforced concrete beams under fatigue loads. *China Civil Engineering Journal*, 45, 118–114.
17. Yang, S., Fang, C. Q., Yuan, Z. J., Yi, M. Y. (2015). Effects of reinforcement corrosion and repeated loads on performance of reinforced concrete beam. *Advances in Structural Engineering*, 18(8), 1257–1272. DOI 10.1260/1369-4332.18.8.1257.
18. Yi, W. J., Sun, X. D. (2007). Experimental investigation on the fatigue behavior of corroded RC beams. *China Civil Engineering Journal*, 40, 6–10.
19. Zhang, W. P., Ye, Z. W., Gu, X. L., Liu, X. G., Li, S. B. (2017). Assessment of fatigue life for corroded reinforced concrete beams under uniaxial bending. *Journal of Structural Engineering*, 143(7), 1–14. DOI 10.1016/j.engstruct.2017.04.005.
20. Andrade, C., Garces, P., Martinez, I. (2008). Galvanic currents and corrosion rates of reinforcements measured in cells simulating different pitting areas caused by chloride attack in sodium hydroxide. *Corrosion Science*, 50(10), 2959–2964. DOI 10.1016/j.corsci.2008.07.013.
21. Abdullah, S., Beden, S. M., Ariffin, A. K., Al-Asady, N. A. (2009). Fatigue crack growth modelling of aluminium alloy under constant and variable amplitude loadings. *Structural Durability & Health Monitoring*, 5(2), 109–131.
22. Su, L. W., Cai, J., Liu, P. G., Chen, Q. J., Wei, M. Y. et al. (2017). Experimental investigation into RC beam under the action of alternating load in salt-spray environment. *Journal of South China University of Technology (Natural Science Edition)*, 45(5), 97–104.
23. Wang, H. C., Gong, J. X., Song, Y. C. (2004). Experimental study on corrosion fatigue of RC beams. *Journal of Building Structures*, 25, 105–111.
24. Yang, L., Sun, L. J. (2015). Damage of steel bar of reinforced concrete bridge by the coupling effect of corrosion and fatigue. *Journal of Tongji University (Natural Science)*, 43(12), 1787–1800.
25. Yin, X. Q. (2015). *Experimental study on fatigue performance of beams under alternating load coupling with corrosive environment (Master's Thesis)*. North China University of Technology, China.